Supporting Information

Formation and Structure of Wild Type Huntingtin Exon-1 Fibrils

J. Mario Isas, Andreas Langen, Myles C. Isas, Nitin K. Pandey, and Ansgar B. Siemer*
Department of Biochemistry and Molecular Medicine, Zilkha Neurogenetic Institute, Keck School of Medicine, University of Southern California

*Corresponding author: 1501 San Pablo Street, Los Angeles, California 90033, United States; Phone: 323 442 2720; Email: asiemer@usc.edu

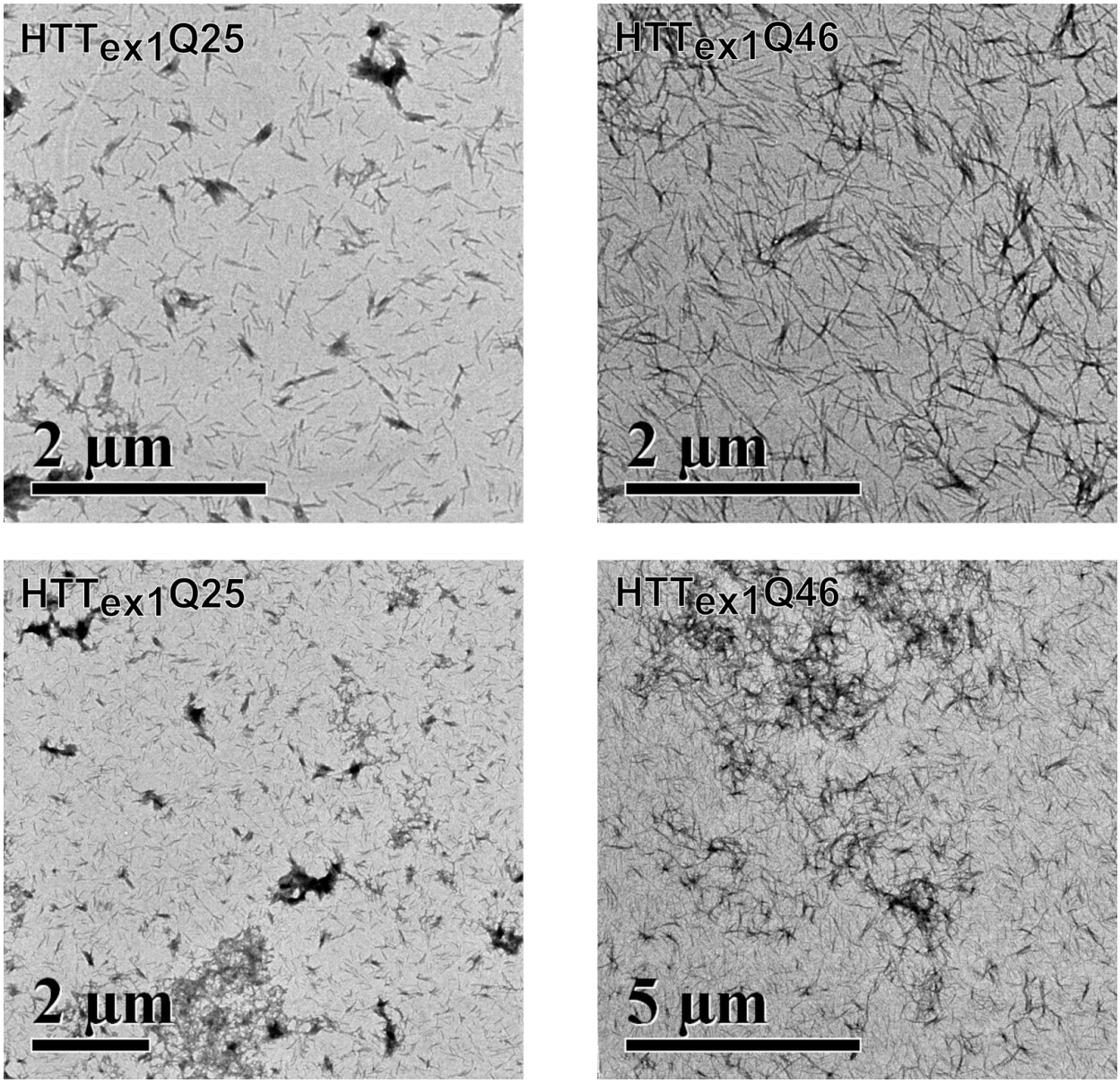

Figure S1: Electron micrographs supplemental to Figure 1 of negatively stained fibrils formed by $HTT_{ex1}Q25$ and $HTT_{ex1}Q46$ in the presence of 5% $HTT_{ex1}Q46$ fibril seeds grown for 24h at 4ºC. $HTT_{ex1}Q25$ fibrils are shorter than the comparable $HTT_{ex1}Q46$ fibrils.

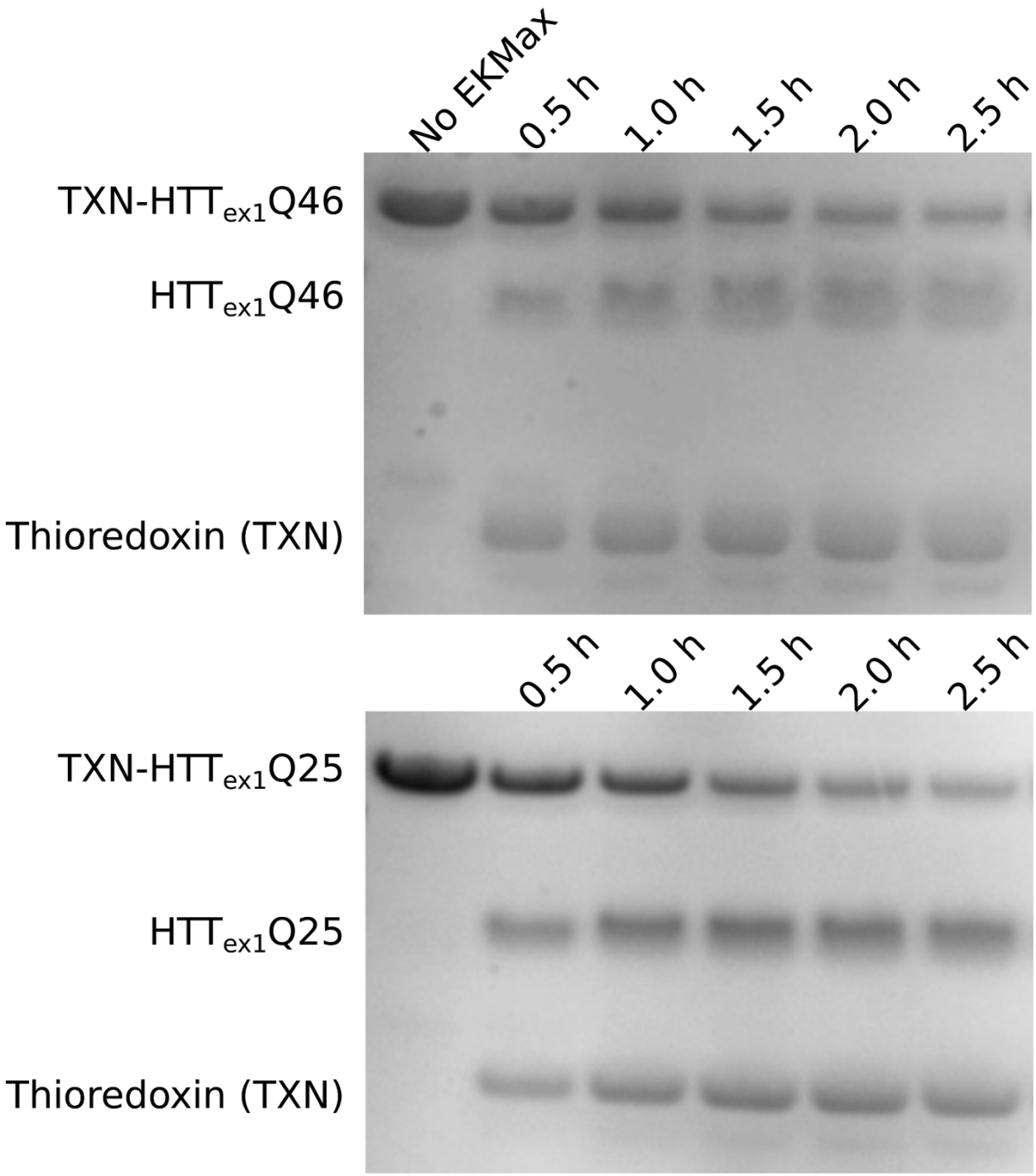

Figure S2: EKMax digestion of thioredoxin tagged HTT$_{ex1}$ Q25 and Q46. SDS page of sample before and at different time points after adding 1 unit EKMax per 280 µg of fusion protein. The bands corresponding to the intact fusion protein, HTT$_{ex1}$, and thioredoxin are indicated for HTT$_{ex1}$Q46 (top) and HTT$_{ex1}$Q25 (bottom). After 2.5 h the majority of the fusion protein has been digested in both cases.

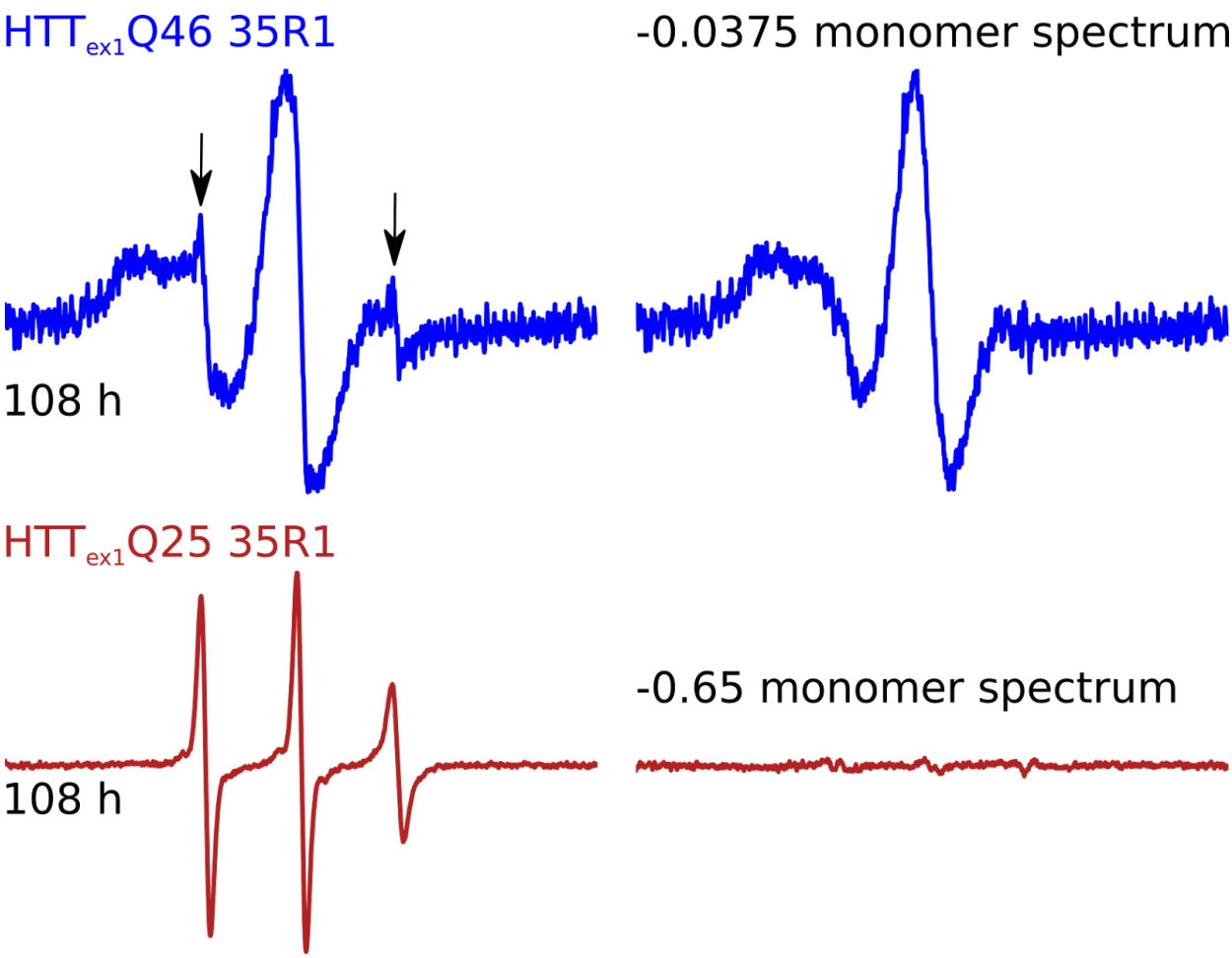

Figure S3: Measurement of equilibrium monomer concentration from the EPR spectra of Figure 3. The EPR spectra of the monomeric state at 0 h were scaled and subtracted from the spectrum after 108 h so that the sharp component, corresponding to the monomer, was minimized. The measured scaling factors and the total protein concentration of 25 μM resulted in equilibrium monomer concentrations of 0.94 μM and 16.25 μM for $HTT_{ex1}Q46$ and $HTT_{ex1}Q25$, respectively.

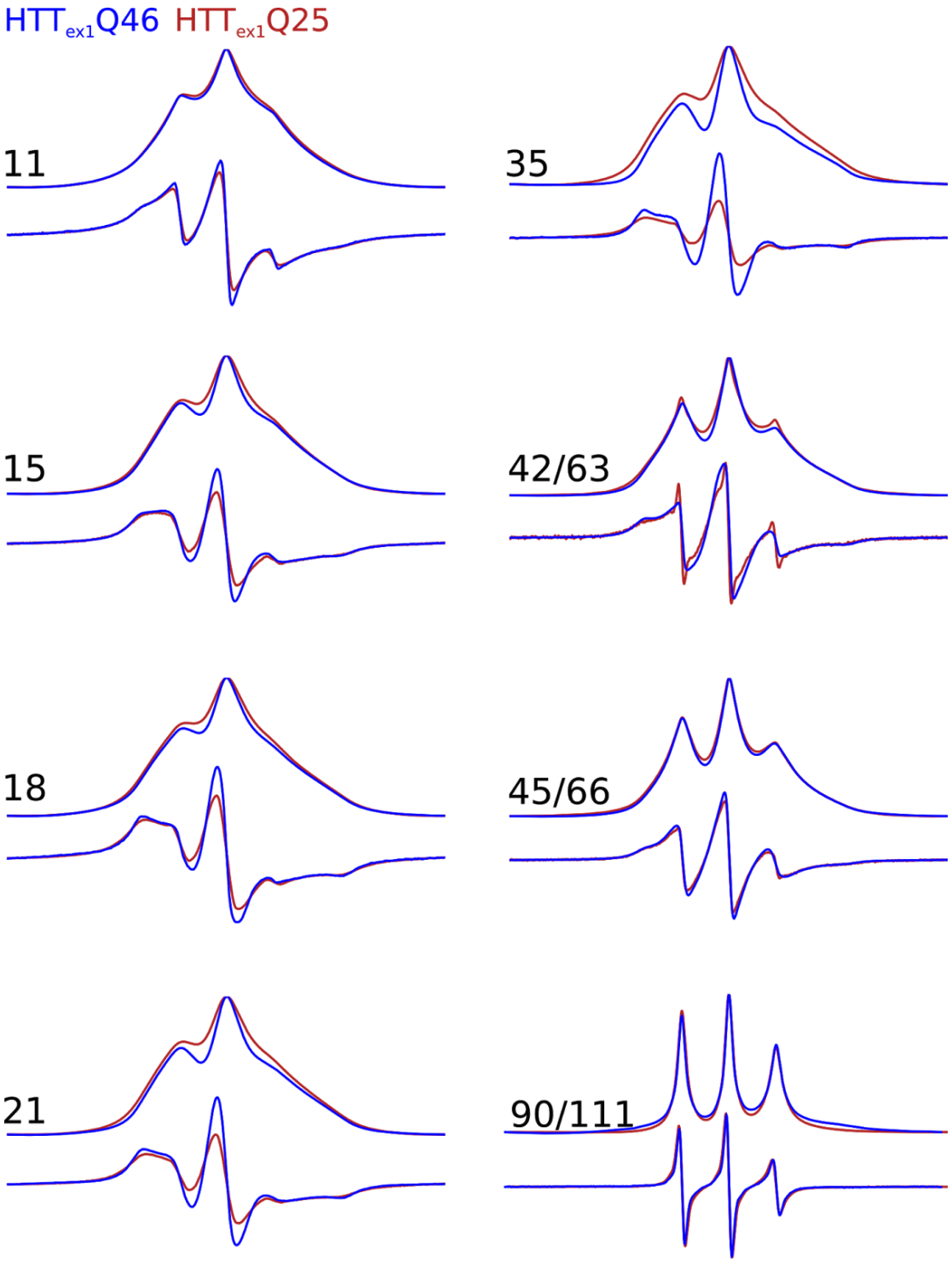

Figure S4: EPR spectra of HTT_{ex1}Q46 and Q25 that were shown in Figure 6 plotted as 1st integral (top) and normalized to the same number of spins (bottom) to illustrate their similarities and differences. The integral shows broader lines for some of the HTT_{ex1}Q25 samples (i.e. 15R1–42R1). In the EPR spectra normalized to the same number of spins, the broader lines translate into a decrease of the overall intensity of the corresponding HTT_{ex1}Q25 spectra.

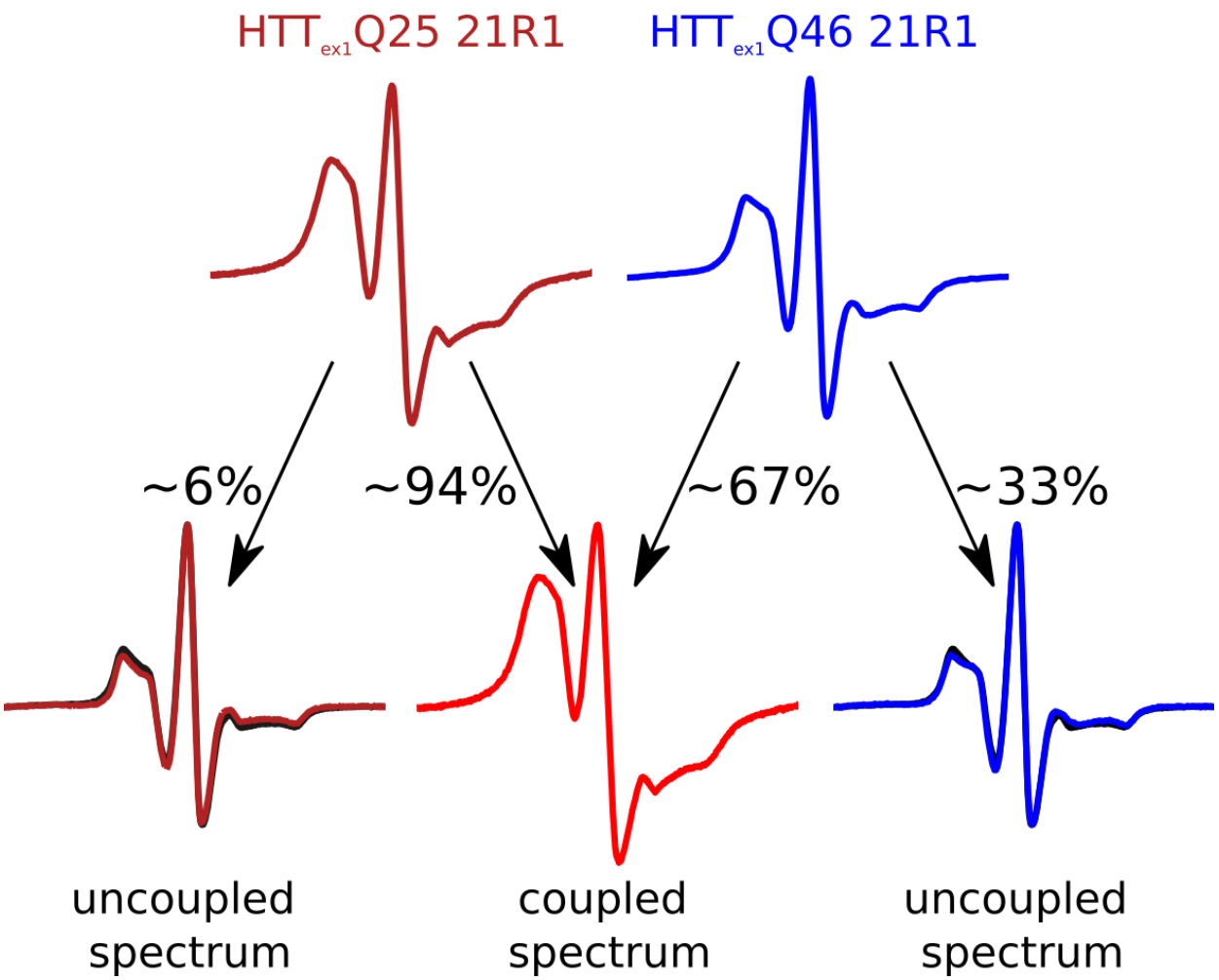

Figure S5: The EPR spectrum of HTT$_{ex1}$Q25 21R1 has a larger spin-spin coupling component compared to HTT$_{ex1}$Q46 21R1. The EPR spectra of HTT$_{ex1}$Q25 and HTT$_{ex1}$Q46 R21 are shown on top. Both spectra are composed of an uncoupled component, corresponding to the EPR spectrum of the 10% MTSL labeled HTT$_{ex1}$Q25 21R1 shown in black at the bottom, and a coupled component shown in red that was determined by subtracting the HTT$_{ex1}$Q46 21R1 from the HTT$_{ex1}$Q25 21R1 spectrum. Consequently, both spectra were deconvoluted using the coupled and uncoupled component showing that the spectrum of HTT$_{ex1}$Q25 21R1 is overwhelmingly dominated by spin-spin coupling, whereas about a third of the spins in HTT$_{ex1}$Q46 21R1 fibrils are uncoupled.